Tungsten: An option for divertor and main chamber plasma facing components in future fusion devices

R. Neu[1], R. Dux[1], A. Kallenbach[1], C.F. Maggi[1], T. Pütterich[1], M. Balden[1], T. Eich[1], J.C. Fuchs[1], O. Gruber[1], A. Herrmann[1], H. Maier[1], H.W. Müller[1], M. O'Mullane[2], R. Pugno[1], I. Radivojevic[1], V. Rohde[1], A.C.C. Sips[1], W. Suttrop[1], A. Whiteford[2], M.Y. Ye[1] and the ASDEX Upgrade team

[1]Max-Planck-Institut für Plasmaphysik, EURATOM Association, D-85748 Garching
[2]Department of Physics, University of Strathclyde, Glasgow
e-mail: Rudolf.Neu@ipp.mpg.de

Abstract   The tungsten programme in ASDEX Upgrade is pursued towards a full high-Z device. The spectroscopic diagnostic and the cooling factor of W have been extended and refined. The W-coated surfaces represent now a fraction of 65 % (24.8 m^2). The only two major components which are not yet coated are the strikepoint region of the lower divertor as well as the limiters at the low field side. While extending the W surfaces, the W concentration and the discharge behaviour have changed gradually pointing to critical issues when operating with a W wall: anomalous transport in the plasma centre should not be too low, otherwise neoclassical accumulation can occur. A very successful remedy is the addition of central RF heating at the 20 - 30% level. Regimes with low ELM activity show increased impurity concentration over the whole plasma radius. These discharges can be cured by increasing the ELM frequency through pellet ELM pacemaking or by higher heating power. Moderate gas puffing also mitigates the impurity influx and penetration, however at the expense of lower confinement. The erosion yield at the low field side guard limiter can be as high as 10^{-3} and fast particle losses from NBI were identified to contribute a significant part to the W sputtering. Discharges run in the upper, W coated divertor do not show higher W concentrations than comparable discharges in the lower C-based divertor.

1. Introduction

A future fusion reactor will have to use high-Z plasma facing components (PFCs) in order to provide low enough erosion and to avoid unduly high co-deposition of tritium with carbon [1]. At present the next step device - ITER - takes a conservative approach using a material mix of Be in the main chamber, W at the divertor baffles and C at the strikepoints. The rationales behind this choice are: the different demands set by the plasma wall interaction at the different positions, the benign behaviour of Be in the main plasma and the advantageous thermo-mechanical properties of C (CFC). However, the still unsolved problem of T co-deposition may lead to the need of exchanging the CFC components before injecting T into ITER. Additionally, probably at a later phase of the ITER operation, all PFCs have to be transformed into high-Z

Figure 1: *View into the upper divertor of ASDEX Upgrade. The graphite tiles were coated by 4 μm of W deposited by PVD. The central column and the upper passive stabiliser loop were already coated previously by 1 μm W.*

components in order to provide operational data for a reactor. ASDEX Upgrade has implemented a W programme, in order to prepare for the decisions which have to be made for ITER and beyond. After the successful operation with a full W divertor in 1995/1996 (W DivI) [2], ASDEX Upgrade has pursued the progressive increase of W PFCs in the main chamber since 1999 [3]. Although the extrapolation to a much larger device may not be straightforward, valuable benchmarks for modelling the implications of high-Z PFCs in a reactor are being gained.

2.   Technical implementation of the W-programme

2.1.   Extension of W-surfaces and Diagnostics   Since the 19th IAEA conference (see [4]) ASDEX Upgrade has substantially increased its W PFCs. For the 2002/2003 campaign the complete central column (heat shield, HS), the inner baffle of the lower divertor (DB) and the upper passive stabiliser loop (PSL) have been covered with new tiles coated by 1 μm of tungsten. Another 10.2 m^2 of W coated PFCs (4 μm) have been installed before the 2003/2004 campaign. One major component, which was coated recently to W, is the upper divertor, shown in Fig. 1. Besides this, the outer baffle at the lower divertor was also W coated. Additionally, one of the guard limiters at the low field side has been equipped with W coated tiles. In summary, the W surfaces comprise now about 24.8 m^2, representing 65% of all plasma facing components. More than thirty dedicated lines of sight for visible spectroscopy have been implemented in order to quantify the influx from all W surfaces.

2.2.   Tungsten Coatings   The coatings were qualified in preparatory experiments [5] and post mortem analyses of previously installed test tiles [6]. For most of the positions, 1 μm of W was sufficient to guarantee complete coverage and to stand the erosion for several campaigns. Since larger erosion was expected in the divertor region, 4 μm of W were used, deposited by plasma arc deposition at Plansee. On the occasion of an intermediate vent during the 2003/2004 campaign it became evident that a few of the W tiles installed in 2003 exhibited delamination at the tiles side surfaces. Since this was also observed at regions with low or negligible power load, it was attributed to problems in the preparation or the production of the coating. On the main surfaces no delamination appeared, except for very few cases of CFC substrate (see Fig. 2), obviously due to the inhomogeneous surface. Independently, melting of the W layer was found at the tile edges in the strike
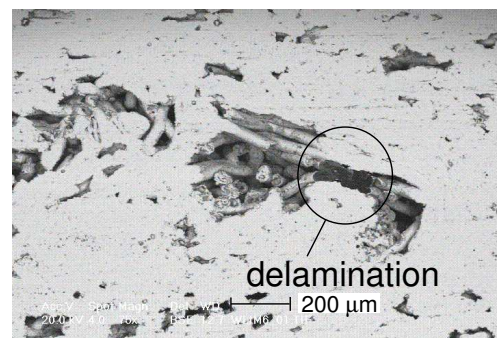

Figure 2: *SEM image of the W coating of a guard limiter tile after exposure to the plasma for one experimental campaign. The W coverage is complete despite the complex CFC surface. The position where delamination occurred is marked by the circle.*

point region of the upper divertor. In contrast to the arrangement chosen for W DivI [2], no tilting of the strikepoint tiles was applied in order to allow for an independent choice of I_p and B_t. As a consequence, the leading edges of the tiles are exposed to a power load which may be higher by a factor of up to 10 compared to the one of the strike zone on the mean surface. None of the tiles was exchanged during the intervention, only loosely bound re-deposited W surface layers were removed. One of the tiles at the low field side guard limiter was investigated by scanning electron microscopy (SEM) analysis using electrons from backscattered electrons (BSE, see Fig. 2), secondary electron emission (SE) and characteristic X-rays (EDX). The tungsten surface appeared almost completely intact and the region where erosion dominated could be identified by their lower low-Z (B, C, O) content. In the deposition dominated zones also significant amounts of Fe, Cr, Ni (stainless steel) were found. Additionally, several melt holes were also found in this area. They are characterised by craters with less than 100μm diameter and edges with increased W thickness. Whether these craters are the footprints of arcs or caused by local overheating due to an insufficient heat contact to the substrate, as it was already observed in laboratory experiments [5], could not be resolved. The W erosion was measured post-mortem X-ray fluorescence analysis. Depending on the position on the tiles an erosion of up to 1.5 μm was detected, which is by far the largest value found for main chamber components.

3. Refinement of diagnostic capabilities and radiation loss parameter

A consistent set of atomic data covering ionisation/recombination coefficients, spectral emission data and corresponding cooling factors for tungsten is still missing. Therefore, a new ADAS [7] extension sets up an infrastructure for all ionisation states with intermediate quality data [8]. Collisional data are calculated using the plane-wave Born approximation (PWB, Cowan code [9]). Although care must be taken in the interpretation of individual spectral lines, the PWB data are very suited for interpreting the radiated power of line arrays. For these, the uncertainties of the individual spectral lines statistically tend to cancel. The calculated excitation rate coefficients, A-values and energy levels are the inputs to a collisional-radiative model where level populations and spectral emissions are derived for different plasma parameters. The abundance of each contributing ion state was calculated using ionisation and recombination data [10] taking transport into account. For the plasma temperatures below 1.7 keV the VUV spectrum is dominated by the well known quasi-continuum at 5 nm, emitted mainly by ionisation states between $W^{27+} \rightarrow W^{35+}$ and it could be simulated satisfactorily. In contrast, the emissions with wavelengths above 5.4 nm could not be reproduced, even when more ion states were included in the modelling. For a hot background plasma (> 2 keV) spectral lines (W^{39+} - W^{45+}) overlay the quasi-continuum emission. These lines were well described by the model.

In the soft X-ray region 90 % of the detectable emission of tungsten below 2 nm is observed between 0.4 nm and 0.8 nm. Comparison to modelled spectra using the new excitation cross sections from ADAS show small deviations in wavelength. As expected, there are differences in the intensity envelope between the measured and modelled spectrum but the basic structure of the emission is well reproduced. Only the strong E2 spectral line at 0.793 nm originating from Ni-like W is strongly underestimated. HULLAC calculations suggest [12] that inner shell ionisation of W^{45+} ($3d^{10}4s^1$) plays a significant role in the level population, a process not yet considered in ADAS. The modelling of the spectral features in the soft X-ray leads to the same W concentration as derived from the total radiation, interpreted with a cooling factor based on ADAS data. In contrast, evaluating the total radiation with data from the average ion model (AIM) [13] results in a concen-

Figure 3: *Cooling factors as a function of plasma temperature from [11] and ADAS; ion abundances as guidelines*

tration which is lower by a factor of 2.5. In Fig. 3 the cooling factors of tungsten from ADAS and the AIM are compared. The lower curve (red) corresponds to the ADAS calculation in which a limited number of configurations is included. To estimate the 'missing' contribution the data were projected to a 'complete' set by extrapolating the included cross sections to higher transitions (black line). The differences between the AIM and ADAS above temperatures of 15 keV are negligible as the amount of continuum radiation becomes comparable to that from line radiation. This vanishing difference indicates that the maximum tolerable tungsten concentration in a reactor or ITER is not altered by this data revision.
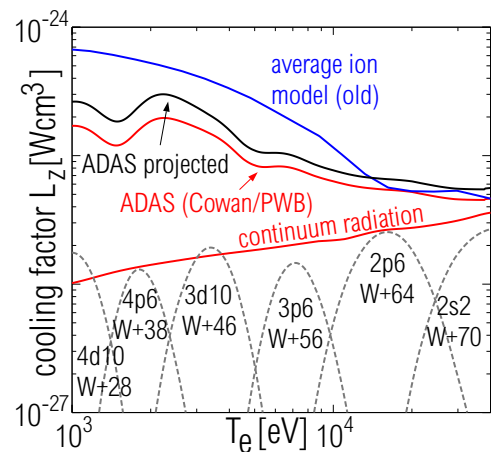
4. W Limiter Erosion

On the route to a full tungsten device, the poloidal limiters have to be transformed to a W surface. Currently, ASDEX Upgrade has 12 poloidal limiters on the low field side: 8 ICRH antenna limiters and 4 guard limiters at the neutral beam ducts. In radial direction, these 4 guard limiters are presently about 12 mm behind the ICRH antenna limiters. Before the tungsten coated tiles were installed at one guard limiter, experiments with a retractable tungsten coated

CFC probe were performed to test the feasibility at this position with enhanced power load [14]. The probe was exposed to a power load above 15 MWm^{-2} and from its characteristic it was concluded that power deposition by fast particles from NBI plays a significant role.

The larger erosion at the limiter (see Sec. 2.2) allowed for spectroscopic tungsten influx measurements [15] by monitoring the WI line radiation at 400.8 nm. The Balmer-δ transition at 410.1 nm was used to calculate the deuterium influx. The measured photon fluxes were transformed into ion fluxes via inverse photon efficiencies [16,7], applying a correction for the larger spatial spread of D_δ [15]. The measured W influx densities Γ_W show a wide variation from below the detection limit ($\approx 2 \times 10^{17}$ m^{-2}s^{-1}) in ohmically and ECR heated discharges to values of $\Gamma_W \approx 10^{19}$ m^{-2}s^{-1} in plasmas with ICRH or NBI heating. Transiently, even higher values of $\Gamma_W = 8 \times 10^{19}$ m^{-2}s^{-1} occur, when the separatrix is very close to the limiter. Γ_W has a strong dependence on the distance between limiter and separatrix, with a decay length of about $\lambda = 1.5$ cm [15]. The quantity $Y_{eff} = \Gamma_W / \Gamma_D$ is an effective erosion yield, which includes the sputtering by deuterium as well as by plasma impurities like carbon and oxygen. It varies from below 10^{-5} to about 2×10^{-3}, and approaches 10^{-2} for transient phases. Fig. 4 shows the temporal evolution of the influxes Γ_W, Γ_D and Y_{eff} in a discharge with a continuous shift towards the low field side limiters for all five lines of sight directed to the different W tiles. Depending on their position Γ_W and Y_{eff} strongly increase. The reduction in Γ_D observed for one channel (black) can be attributed to reduced D recycling at the central column. To interpret the yields, a knowledge of the energy spectrum of the incident

Figure 4: *Time traces for discharge #18740 ($I_p = 1$ MA, $B_t = -2.5$ T) with a radial shift towards the low field side guard limiter. From top to bottom: effective sputtering yield Y_{eff}, W- and the H-fluxes Γ_W, Γ_D at the different W limiter tiles, their distance to the separatrix ΔR_{sep}, heating power from NBI and ICRH and D_α.*

ions is needed. From thermocouple measurements and Γ_D the average deposited energy per deuterium ion can be calculated for discharges with long steady state phases. It turns out that the measured Y_{eff} can only be explained by the contribution of a considerable amount ($\approx 5\%$) of fast particles from auxiliary heating [15].

5. Operation with W Divertor

The discharges run with upper single null (USN) comprise ordinary L- and H-modes as well as plasmas with high β_N. Discharges with low power NBI heating show increased W concentrations (c_W), but in most scenarios there is no obvious difference with discharges run in the lower (C based) divertor (LSN). Even during a continuous transition from USN to LSN no significant change in the W content could be identified [15].

Due to the low pumping capacity (there are no pumps in the upper divertor which could benefit from the higher neutral pressure in the divertor chamber) and the limited power load capability of the coated tiles (see Sec. 2.2) it was not possible to run low density improved H-Modes in USN. However, discharges at higher density and high heating power were performed, investigating their behaviour at high β_N. The main parameters of such a discharge are depicted in Fig. 5. Although the confinement is not as good as in its LSN counterpart [17] $\beta_N = 2.8$ at an H-factor $H_{98,y2} = 0.95$ is reached, combined with the low W concentration $c_W \leq 2 \cdot 10^6$, which is constant throughout the divertor phase.
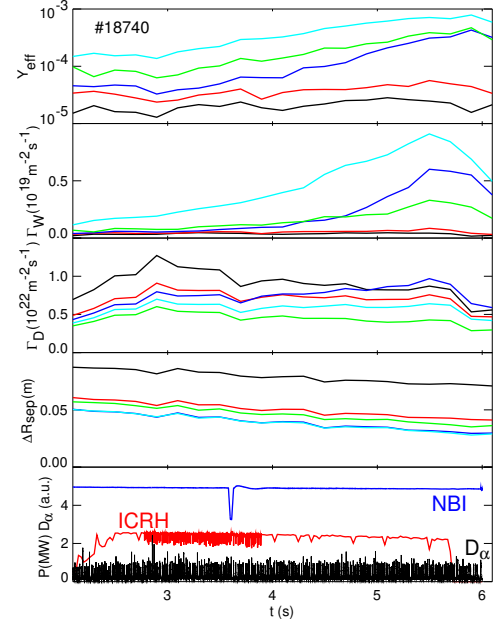
In ordinary hydrogen discharges no W above the detection limit of about $2 \cdot 10^{-7}$ was observed. The reason may be found in the reduced source due to the lower sputtering rate. This could not be proven experimentally since the W I flux in the upper divertor was usually below the detection limit. However, since light impurities are found to dominate the W-sputtering yield (see [16]) some reduction of the W source is expected due to the lower C contamination usually observed in hydrogen discharges. Additionally, the lower confinement and the higher ELM frequency may lead to the strongly reduced W concentrations. This point should be taken into account when extrapolating from the hydrogen phase in a next step device. It should be noted that the discharge where melting at the leading edges occurred (# 18376, see Sec. 2.2), occurred before the above discussed discharges.

6. Compatibility with plasma scenarios
6.1. Long-term evolution of W-concentrations
The simplest way to investigate the long term evolution of the W concentration is to evaluate it in identical ohmic discharges. Although the discharges and their W concentrations themselves are not relevant, they allow to eliminate the strong influence of the transport observed in additionally heated plasmas. In ASDEX Upgrade, every day of operation starts with an identical ohmic discharge at $I_p = 800$ kA, $B_t = -2$ T and $q_{95} = 4$. There are two different density levels namely $n_e = 2.5 \cdot 10^{19}$ m^{-3} and $n_e = 3.5 \cdot 10^{19}$ m^{-3}. In the second phase the level of W is always at or below the detection limit $2 \cdot 10^{-7}$, whereas signatures of W are visible during the low density phase. During discharges run through 2002, typical W concentrations of $5 \cdot 10^{-7}$ were observed, periodically reduced by a factor of 2-4 for about 50-100 consecutive discharges after boronisations. At that time the central heat shield was W-coated, representing 7.1 m^2. With the increasing W coverage also the W concentration has risen. At present, usually $c_W = 2 - 3 \cdot 10^{-6}$ is observed, i.e. an increase by a factor of about 5. As expected, this increase is larger than the increase in surface area (7.1 m$^2 \rightarrow$ 24.8 m^2) pointing to the fact that there are regions with higher source rate/ penetration probability than the central column installed during 2002. From post mortem erosion

Figure 5: *Time traces for the USN discharge #19424 ($I_P = 800$ kA, $B_t = 2.0$ T) with a continuous rise of the auxiliary heating power. The discharge is terminated by a safety interlock to prevent from overloading the upper W target-plates.*

measurements [18,19] and influx measurements (see Sec. 4) one can identify the outer lower divertor baffle, the upper PSL (which for low δ discharges can be as close to the separatrix as the limiters) and the W coated guard limiter, as important W sources.

A similar increase of c_W is also found in the so called standard H-Mode discharge $I_p = 1$ MA, $B_t = -2$ T and $q_{95} = 3.2$ [20] also performed daily. Here c_W increased from $\approx 10^{-6}$ to $\approx 10^{-5}$ during the low heating ($P_{aux} = 2.5$ MW) natural density. However, since this phase exhibits a very good particle confinement combined with the feedback loop described below (Sec. 6.2), only the very first stage can be used for this kind of evaluation. In a later phase of the discharge, when the density and the heating power are increased ($P_{aux} = 5$ MW, $n_e = 10^{20}$ m^{-3}), c_W is always $\ll 10^{-6}$. Both discharge types confirm the general observation, that the W concentration is strongly reduced by changing the edge parameters through gas puffing. In addition, hints for
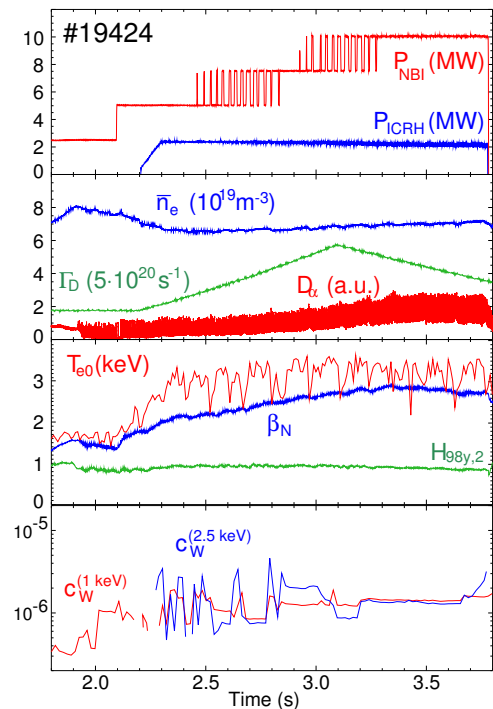
a long term change of the edge parameters are found from the increase of plasma temperatures at the outer divertor inferred from thermo-currents. This points to a reduction of the edge radiation, although the central C concentrations did not change significantly and remained around $1 - 2\%$.

6.2.   Conventional H-Mode discharges   In contrast to operation in an 'all-carbon' device, there is a strong difference between W-limiter and divertor operation. This was documented in a discharge with divertor → W inner limiter → divertor transitions under otherwise similar discharge conditions. The W concentration increased by a factor of 100 ($10^{-5} \rightarrow 10^{-3}$) when losing the divertor X-point and the strong bulk W-contamination was again suppressed after the backtransition to divertor configuration [21]. This behaviour demonstrated also that the W-surfaces are visible to the plasma still after half a year of operation, in line with the post mortem analysis of W-tiles [18]. The W-influx from the HS was estimated from Langmuir probe data using the yields measured during the W-divertor experiment [16]. During the divertor phase temperatures of $T_e \approx 6$ eV connected to electron densities below 10^{18} m^{-3} are observed, yielding W-influxes $\Gamma_W \leq 4 \cdot 10^{17}$ s^{-1}m^{-2}. As soon as the separatrix is lost the temperature and density rise, leading to $\Gamma_W \approx 3 \cdot 10^{19}$ s^{-1}m^{-2}, i.e. a similar increase as for c_W.

A critical parameter for the W inventory is the transport near the edge as has been known for a long time from ELM-free H-Modes. Additionally, there is the indication for a feed back loop, which leads to an unstable situation in the case of operation near the L-H threshold. Here, the ELM-frequency is low and during the time in-between ELMs, impurities penetrate much more easily into the plasma [22], leading to increased impurity concentration and radiation. In contrast to C, which under normal plasma conditions mostly radiates in the SOL, a substantial amount of power is radiated inside the separatrix when heavier species (mid-Z as well as W, both observed in ASDEX Upgrade) are involved. This leads to a reduced power flux crossing the pedestal region and consequently results in a lower ELM frequency, closing the feedback loop. Such a behaviour is observed

Figure 6: *Tungsten sputtering yields for different species versus plasma temperature, assuming $E_{impact} = 3ZT + 2T$. Total yields are multiplied by the assumed concentrations to obtain realistic, effective yields per fuel ion flux. Charge states used for the calculation are given in the inset.*

in the long term evolution in the low heating phase (2.5 MW of NBI) of the 'standard H-Mode' discharge. There, at the front end of the discharge, the ELM-free period is prolonged from day to day ultimately getting ELM free and eventually leading to a radiation collapse. A remedy is to increase the heating power, which keeps up the ELM frequency and lowers considerably the W content [21]. Another possibility to break the self-amplifying cycle is to enforce ELM activity by pellet injection in a similar way to the procedure described in [23,24] aimed to the set-up of an integrated exhaust scenario including edge cooling by seeded impurities. Special emphasis is devoted to these investigations since a future carbon free device will crucially depend on radiation cooling in order to mitigate the divertor power load. Experiments with argon seeding resulted in a significant reduction of the divertor electron temperature, while keeping the W and Ar central density low by applying central RF heating and ELM pace-making. An obvious question is whether impurity seeding leads to a higher W source due to more efficient sputtering by heavier species impinging at a potentially higher charge state. Earlier experiments
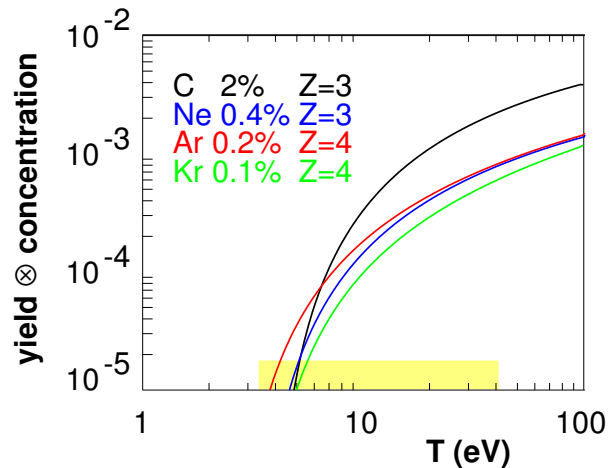
with Ne seeding in with the W DivI [16] showed that even a reduction of the W influx could be achieved. Due to the low W flux densities from the wall, this question could not yet be re-addressed experimentally. However, tungsten sputtering yields can be calculated from [25] using estimated concentrations and charge states in a realistic scenario. This means that the plasma impurity concentration is assumed to vary with 1/Z, since the main plasma $\Delta P_{rad}/\Delta Z_{eff}$ rises with the impurity charge [23]. As can be judged from Fig. 6, there is virtually no difference in W sputtering yields for Ne, Ar and Kr at their corresponding (ITER relevant) concentration in the range of typical SOL and divertor temperatures. In contrast, carbon leads the highest sputtered W flux in this assessment.

6.3. Improved H-Modes and ITBs   Since improved H-Modes usually show a significantly higher density peaking than conventional H-Modes, they are more prone to central W accumulation. Indeed a peaking of the W density of up to a factor 60 was observed in NBI only heated discharges. The W accumulation can be suppressed significantly by central RF heating (ECRH,ICRH) at a level of 30% of the total auxiliary heating power. Experiments with trace impurities [26,27] reveal that this reduction is due to the twofold effect of an increase of the anomalous transport as well as the reduction of the neoclassical inward drift. It is important to note, that the performance ($H_{98}\beta$) of the discharges is only reduced by less than 10% as it could be shown in systematic studies [28,17].

Tungsten contamination does not play a role in the investigation of the ITB scenarios when using a divertor configuration. Typically concentrations in the range of 10^{-5} are observed. However, their usual lifetime of a few hundred milliseconds is much shorter than the rise-time for central accumulation observed in steady state discharges with low central transport.

7. Discussion and Outlook

The tungsten programme in ASDEX Upgrade is pursued vigorously towards a full high-Z device. The W-coated surfaces represent now a a fraction of 65 % (24.8 m^2) and the only two major components which are not yet coated are the strikepoint region of the lower divertor and the limiters at the low field side. The spectroscopic diagnostic and the cooling factor of W were extended and refined within the framework of ADAS. It yields a significant reduction of the cooling factor in the temperature range of 1 to 5 keV. Since the W coating of the central column the W concentration and the discharge behaviour have changed gradually pointing to critical issues when operating with a W wall: transport in the plasma centre should not be too low, otherwise neoclassical accumulation can occur. The overall behaviour of this kind of discharges is often not influenced at all, because the accumulation occurs only in the very centre and it plays only a minor role in the global power balance. A very successful remedy is the addition of central RF heating at the 20 - 30% level. The other issue is founded in the behaviour of the plasma edge: regimes with low ELM frequency show increased W concentration. From the viewpoint of operation this issue is severer than the first one, since the impurity content rises over the whole plasma radius leading to strong radiation or even radiation instability. The discharges can be cured by increasing the ELM frequency trough pellet ELM pacemaking or by higher heating power. Moderate gas puffing can also mitigate the impurity influx and penetration, however at the expense of lower confinement. Another observation pointing in the same direction is the very low W content found in discharges with higher fractions of hydrogen (H > 10%), as they usually show higher ELM frequency. The erosion yield at the low field side guard limiter can be as high as 10^{-3} and fast particle losses from NBI were identified to contribute a significant part to the W sputtering. Discharges run in the upper, W coated divertor do not show higher W concentrations than comparable discharges in the lower C-based divertor.

For the upcoming 2004/2005 campaign a further extension of the W surfaces is envisaged. This comprises mainly structures at the low field, side as there are 39 auxiliary limiters in between the outer upper divertor and the upper PSL (see Fig. 1) as well as the guard limiters which are

redesigned to stand higher heat fluxes. Additionally, one of the ICRH limiters will be W coated to study the influence of fast particles produced by sheath rectification at the antennas. The tiles for both limiter types are manufactured from graphite instead of CFC in order to get a more homogeneous surface. They are coated by plasma spray to a thickness of 200 μm to assure sufficient lifetime.

The extrapolation to ITER or DEMO remains difficult. However none of the above measures seems to be incompatible with the aspired standard operation scenarios. Simulations using the predicted central background thermal transport in ITER look very promising as long as the central diffusivity stays above $0.01 m^2 s^{-1}$ and an anomalous drift parameter v/D does not depend positively on Z [27]. For the edge behaviour the situation is less clear, since the W penetration is governed by the complex interplay of radial and parallel transport. However the operation with strong low frequency ELMs is also not acceptable from the target lifetime point of view for any material [29]. After all, the question whether W PFCs are suited for specific plasma scenarios may have to be rephrased to the question of which plasma scenarios are compatible with tungsten considering the lack of alternatives to high-Z PFCs in a reactor.

References

[1] BOLT, H. et al., J. Nucl. Mater. **329-333** (2004) 66.

[2] NEU, R. et al., Plasma Phys. Controlled Fusion **38** (1996) A165.

[3] NEU, R. et al., Fusion Eng. Design **65** (2003) 367.

[4] ROHDE, V. et al., *Proc. of the 19th IAEA Conference Fusion Energy (CD-Rom), Lyon, France, October 2002*, volume IAEA-CSP-19/CD, pages IAEA–CN–94/EX/D1–4, Vienna, 2003, IAEA.

[5] MAIER, H., to appear in Materials Science Forum **475-479** (2005) 1377.

[6] KRIEGER, K. et al., J. Nucl. Mater. **313–316** (2003) 327.

[7] SUMMERS, H. P., Atomic data and analysis structure users manual, JET-IR 06 (1994).

[8] PÜTTERICH, T. et al., *Proc. of the 31st EPS Conference on Plasma Physics and Controlled Fusion, London, 2004*, pages P–4.116, Geneva, 2004, EPS.

[9] COWAN, R., The theory of atomic structure and spectra, in *Univ. of Calif. Press*, 1981.

[10] ASMUSSEN, K. et al., Nucl. Fusion **38** (1998) 967.

[11] POST, D. et al., At. Data Nucl. Data Tables **20** (1977) 397.

[12] FOURNIER, K. et al., *Bulletin of the American Physical Society*, volume 46, page 267, 2001.

[13] POST, D. et al., Phys. Plasmas **2** (1995) 2328 .

[14] YE, M.Y. et al., PSI 2004, Portland, to appear in J. Nucl. Mater. (2004).

[15] DUX, R. et al., PSI 2004, Portland, to appear in J. Nucl. Mater. (2004).

[16] THOMA, A. et al., Plasma Phys. Controlled Fusion **39** (1997) 1487.

[17] STÄBLER, A. et al., *this conference*.

[18] KRIEGER, K. et al., PSI 2004, Portland, to appear in J. Nucl. Mater. (2004).

[19] MAIER, H. et al., to appear in J. Nucl. Mater. (2004).

[20] RYTER, F. et al., Plasma Phys. Controlled Fusion **44** (2002) A407.

[21] NEU, R. et al., Proc. of the 30th EPS Conference on Controlled Fusion and Plasma Physics, St. Petersburg, 2003 (CD-ROM), edited by KOCH, R. et al., volume 27A, pages P–1.123, Geneva, 2003, EPS.

[22] DUX, R., Fusion Science and Technology **44** (2003) 708.

[23] KALLENBACH, A. et al., PSI 2004, Portland, to appear in J. Nucl. Mater. (2004).

[24] LANG, P. et al., *this conference*.

[25] ECKSTEIN, W. et al., Nucl. Instr. Meth. **B83** (1993) 95.

[26] DUX, R. et al., Plasma Phys. Controlled Fusion **45** (2003) 1815.

[27] DUX, R. et al., *this conference*.

[28] MAGGI, C. et al., *Proc. of the 31st EPS Conference on Plasma Physics and Controlled Fusion, London, 2004*, pages P–4.119, Geneva, 2004, EPS.

[29] FEDERICI, G. et al., J. Nucl. Mater. **313–316** (2003) 11.